

Cite this: *Catal. Sci. Technol.*, 2024,  
14, 6947

# Selectively controlled synthesis of diethyl carbonate and methyl ethyl carbonate *via* transesterification of dimethyl carbonate over a KATriz/Al<sub>2</sub>O<sub>3</sub> catalyst†

Peixue Wang, ‡<sup>ab</sup> Shimin Liu, ‡<sup>a</sup> Xinjiang Cui \*<sup>ab</sup> and Feng Shi \*<sup>ab</sup>

In this work, a series of Al<sub>2</sub>O<sub>3</sub>-supported KATriz (3-amino-1,2,4-triazole potassium) catalysts were developed and employed for the transesterification of dimethyl carbonate (DMC) with ethanol to synthesize diethyl carbonate (DEC) and methyl ethyl carbonate (EMC). It turned out that the 14 wt% KATriz/Al<sub>2</sub>O<sub>3</sub> catalyst displayed high activity and possessed adjustability for selective conversion to DEC or EMC *via* varying the molar ratio of ethanol to DMC. Under optimized conditions, the selectivity of DEC reached 91% when the ratio of DMC to ethanol was 1:10. Meanwhile, the selectivity of EMC reached up to 99% when the ratio was 4:1, and the catalyst remained stable after a time on stream of 500 h. The prepared catalysts were characterized by BET, TG, XRD, IR, XPS and TPD to establish the relationship between structure and performance. XPS results indicated a significant interaction between KATriz and Al<sub>2</sub>O<sub>3</sub>, and TPD results showed that 14 wt% KATriz/Al<sub>2</sub>O<sub>3</sub> with more accessible basic sites were beneficial for excellent catalytic performance.

Received 12th August 2024,  
Accepted 12th October 2024

DOI: 10.1039/d4cy00979g

rsc.li/catalysis

## 1. Introduction

Diethyl carbonate (DEC) and ethyl methyl carbonate (EMC) are important reaction intermediates, and their molecular structures contain carbonyl and ethyl groups, which can serve as carbonylation or alkylating agents. Moreover, they are widely used in lithium-ion batteries and fuel additives due to their high dielectric constant, low viscosity, and fine solubility for Li salts.<sup>1,2</sup> At present, several methods have been reported for DEC and EMC synthesis. The phosgene method takes on high production efficiency, but the starting material phosgene is extremely toxic and the process produces strong acidic HCl, which seriously corrodes the equipment.<sup>3,4</sup> Hence such a method has gradually been phased out. The oxidative carbonylation method utilizes methanol, ethanol, CO, and O<sub>2</sub> as the main raw materials, but the EMC yield is too low and the involved O<sub>2</sub> in the reaction causes a safety hazard.<sup>5,6</sup> Additionally, the synthesis of EMC *via* transesterification from

DMC is considered a benign route, which has the advantages of low cost, pollution-free, and mild reaction conditions. Moreover, the byproduct methanol can be recycled for the production of DMC, which is the raw material. As ethanol is excessive, EMC would continue to undergo transesterification to generate DEC, so the ratio of EMC and DEC can be adjusted according to actual needs by changing the raw material ratio. However, the reaction rate is relatively low in this process, so the catalyst plays an important role in increasing the reaction rate and improving the selectivity of EMC or DEC. Thus far, catalysts adopted in this process were mainly homogeneous base catalysts, for example sodium alcoholate and lanthanum nitrate, which are difficult to separate.<sup>7–9</sup> In this context, developing an environmentally friendly heterogeneous catalyst for efficient synthesis of EMC and DEC is crucial. In previous studies, some heterogeneous catalysts for transesterification between DMC and C<sub>2</sub>H<sub>5</sub>OH have been reported (Table 1), but the processes usually suffered from long reaction time or low selectivity in these catalytic systems. Therefore, it is necessary to further utilize heterogeneous catalysts with high catalytic performance and low cost for the industrial synthesis of EMC and DEC.

Al<sub>2</sub>O<sub>3</sub> is a good carrier with many advantages such as low cost, large surface area and high thermal stability for industrial applications.<sup>19,20</sup> The solid base catalyst loaded with potassium active component on Al<sub>2</sub>O<sub>3</sub> can effectively catalyze the transesterification reaction to synthesize organic

<sup>a</sup> State Key Laboratory of Low Carbon Catalysis and Carbon Dioxide Utilization, State Key Laboratory for Oxo Synthesis and Selective Oxidation, Lanzhou Institute of Chemical Physics, Chinese Academy of Sciences, Lanzhou, 730000, China.  
E-mail: fshi@licp.cas.cn; Tel: +86 931 4968142

<sup>b</sup> Qingdao Center of Resource Chemistry & New Materials, Qingdao, 266100, China  
† Electronic supplementary information (ESI) available. See DOI: <https://doi.org/10.1039/d4cy00979g>

‡ Peixue Wang and Shimin Liu are co-first authors.



**Table 1** Summary of the work reported on the synthesis of DEC (EMC) from DMC and C<sub>2</sub>H<sub>5</sub>OH over various catalysts

Catalyst	Operation conditions (temp, time, DMC : C <sub>2</sub> H <sub>5</sub> OH molar ratio, cat. amount)	DMC con. (%)	EMC sel. (%)	DEC sel. (%)	Ref.
Modified K <sub>2</sub> CO <sub>3</sub>	75 °C, 26.6 h, 1 : 2, 7 wt%	26.6	67.1	32.9	10
MOF-808	75 °C, 24 h, 1 : 3, 1 wt%	82.6	60.0	36.2	11
KF/Al <sub>2</sub> O <sub>3</sub>	80 °C, 4 h, 1 : 4, 2 wt%	86.8	45.7	54.3	12
K <sub>2</sub> CO <sub>3</sub> /Al <sub>2</sub> O <sub>3</sub>	140 °C, 1 : 10, WHSV 0.98 h <sup>-1</sup>	97.4	—	79.5	13
Mg–Al–O– <i>t</i> -Bu HT	80 °C, 7 h, 1 : 5, 1 wt%	86.4	25.9	70.8	14
MgO–HZSM-5	90 °C, 7 h, 2.6 : 1, —	89.3 <sup>a</sup>	85.7	—	15
Mg–Al oxides	80 °C, 1 h, 0.8 : 1, 1 wt%	81.7	70.1	29.9	16
DBU–PO@ZIF-8	90 °C, 5 h, 3 : 1, 5 wt%	58.8 <sup>a</sup>	94.7	—	17
MgZnP/AT–ZSM-5	90 °C, 26 h, 3.3 : 1, 3.9 wt%	99.1 <sup>a</sup>	96.3	—	18
14 wt% KATriz/Al <sub>2</sub> O <sub>3</sub>	80 °C, 8 h, 1 : 10, 11 wt%	88	9	91	This work
14 wt% KATriz/Al <sub>2</sub> O <sub>3</sub>	80 °C, 8 h, 3 : 1, 3.7 wt%	19	98	2	This work

<sup>a</sup> C<sub>2</sub>H<sub>5</sub>OH conversion.

carbonates.<sup>21,22</sup> In our previous work, the KATriz catalyst with moderate basic sites displayed excellent performance for transesterification reaction between 1,6-hexanediamine and DMC.<sup>23</sup> Herein, we further developed a range of heterogeneous KATriz/Al<sub>2</sub>O<sub>3</sub> catalysts for the synthesis of DEC and EMC from DMC and C<sub>2</sub>H<sub>5</sub>OH. The reaction was operated both in a batch reactor and a fixed-bed reactor in a liquid–solid mode. Besides, this work also studied the effects of reaction conditions and reusability.

## 2. Experimental

### 2.1 Chemicals

Chemicals including C<sub>2</sub>H<sub>5</sub>OH, DMC, KOH were bought from Sinopharm Chemical Reagent Co., Ltd. 3-Amino-1*H*-1,2,4-triazole (ATriz) was purchased from Shanghai Macklin Biochemical Technology Co., Ltd.

### 2.2 Catalysts preparation

Al<sub>2</sub>O<sub>3</sub>-supported KATriz catalysts were prepared by equal volume impregnation method. First, KATriz was synthesized by stirring a mixture of ATriz and KOH (KOH and ATriz molar ratio of 1 : 1) in deionized water for 12 h. Al<sub>2</sub>O<sub>3</sub> support was added to the KATriz solution prepared above and it was immersed at room temperature for 24 h. The impregnating material was dried at 80 °C for 2 h, and then further dried under vacuum conditions for 3 h at a temperature of 180 °C. The sample was represented as *y* wt% KATriz/Al<sub>2</sub>O<sub>3</sub>, where *y* represented the design weight load of KATriz (*y* = 7, 14, and 20).

### 2.3 Synthesis of DEC and EMC from DMC and C<sub>2</sub>H<sub>5</sub>OH

The batch mode was conducted in a 100 mL round-bottom flask equipped with a spiny fractionating column (20 cm). In the procedure, DMC, C<sub>2</sub>H<sub>5</sub>OH and catalyst were charged in the flask successively, and then the reaction was carried out under strong stirring at the required time and temperature. As the reaction was completed, the reactor was cooled down to room temperature and the solid catalyst was recovered

from the resulting liquid mixture by centrifugation. The filtrate was identified using biphenyl as the internal standard using the HP-6820 GC equipped with an FID detector. The conversion of DMC, yield of DEC and EMC were calculated using the following formulas:

$$C_{\text{DMC}} = \frac{n_{\text{DEC}} + n_{\text{EMC}}}{n_{\text{DMC}}} \times 100\%$$

$$Y_{\text{DEC}} = \frac{n_{\text{DEC}}}{n_{\text{DMC}}} \times 100\%$$

$$Y_{\text{EMC}} = \frac{n_{\text{EMC}}}{n_{\text{DMC}}} \times 100\%$$

Here,  $C_{\text{DMC}}$  is the DMC conversion;  $Y_{\text{DEC}}$  is the DEC yield;  $Y_{\text{EMC}}$  is the yield of EMC;  $n_{\text{DMC}}$  is the moles of DMC in the feed before reaction;  $n_{\text{DEC}}$  is the mole of DEC in the product after reaction,  $n_{\text{EMC}}$  is the mole of EMC in the product after reaction.

In the fixed-bed mode, DMC and C<sub>2</sub>H<sub>5</sub>OH were introduced by using a high-pressure metering pump at a given flow rate and continuously passed the preheating vaporizer and catalyst bed (particle size 2–3 mm), and the reaction was conducted at the set temperature under ordinary pressure. All the products were analyzed using similar procedures as described above.

## 3. Results and discussion

### 3.1 Results of the catalysts characterization

N<sub>2</sub> adsorption–desorption isotherms of the catalysts based on KATriz/Al<sub>2</sub>O<sub>3</sub> (Fig. 1a) showed typical type-IV isotherms for mesoporous materials, with a wide distribution of pore sizes between 5 and 20 nm (Fig. 1b). These mesopores can promote the diffusion of product and reagent molecules. The surface area of the Al<sub>2</sub>O<sub>3</sub> carrier was 155.77 m<sup>2</sup> g<sup>-1</sup> (Table 2). It could be seen that the surface area, the average pore size and the pore volume of the 7 wt% KATriz/Al<sub>2</sub>O<sub>3</sub> and 14 wt%



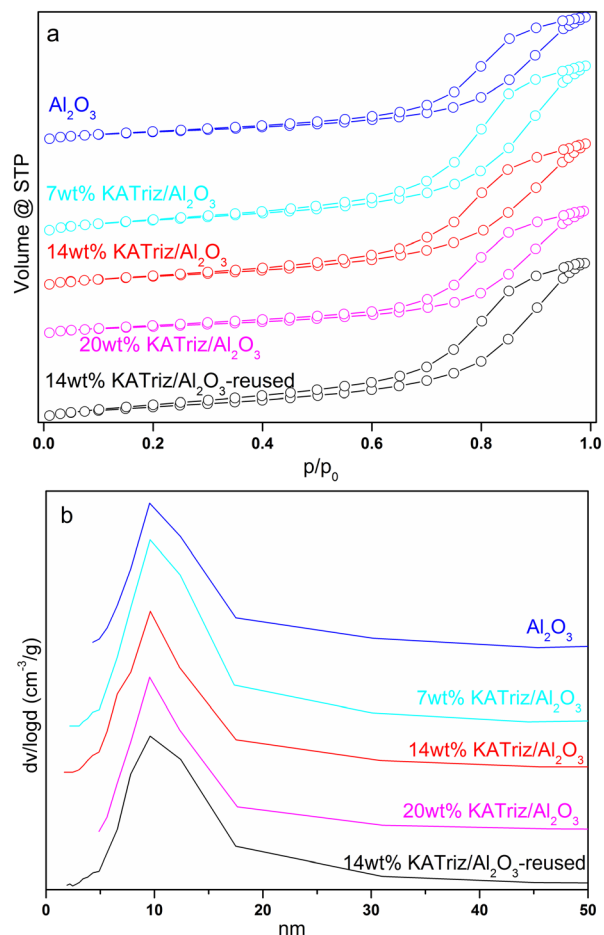


Fig. 1  $N_2$  adsorption isotherms (a) and pore size distributions (b) of the KATriz/ $Al_2O_3$  catalysts.

KATriz/ $Al_2O_3$  catalysts increased, which suggested the diffusion of KATriz into the pores of  $Al_2O_3$  with the new surface structure emerged. The surface area slightly decreased as the content of KATriz was further increased, which was possibly attributed to the aggregation of KATriz and its blocking effect on some pores of  $Al_2O_3$ .

The thermogravimetric (TG) curves of catalysts are shown in Fig. 2. The decomposition process of KATriz could be roughly divided into three sections. There was approximately 8% weight loss before 250 °C, mainly due to the water

adsorbed on the catalyst surface (this salt is highly hygroscopic and deliquescent in air). The next two platforms should be the decomposition of nitrogen-containing heterocycles, and the total weight loss rate was about 71.6% within the temperature range of 30–800 °C. As the temperature increased, the loaded catalyst would undergo a continuous weight-loss process without a weight-loss platform. The final weight loss rates were 7 wt% KATriz/ $Al_2O_3$  (8.6%), 14 wt% KATriz/ $Al_2O_3$  (12.7%), 20 wt% KATriz/ $Al_2O_3$  (14.7%), 14 wt% KATriz/ $Al_2O_3$ -reused (11.4%), which was positively correlated with the loading amount. The weight loss rate of the reused catalysts was slightly lower than that of fresh catalysts due to the loss of KATriz salt adsorbed on the catalyst surface during the reaction process. Apart from the influence of a small amount of adsorbed water, TG results indicated that the catalyst was stable under the reaction conditions.

XRD patterns of KATriz, 14 wt% KATriz/ $Al_2O_3$  and 14 wt% KATriz/ $Al_2O_3$ -reused are shown in Fig. 3. The typical XRD peaks of cubic phase  $\gamma$ - $Al_2O_3$  (JCPDS Card No. 04-0880) at 37.8, 45.8, 67.4° could be observed for 14 wt% KATriz/ $Al_2O_3$  and 14 wt% KATriz/ $Al_2O_3$ -reused.<sup>24</sup> The KATriz XRD signal was not detected in catalysts 14 wt% KATriz/ $Al_2O_3$  and 14 wt% KATriz/ $Al_2O_3$ -reused, which suggested that KATriz nanoparticles dispersed well on the surface of the catalyst. The good dispersibility of KATriz on  $Al_2O_3$  could reduce the dosage of the active components KATriz, which was also one of the reasons for its better activity compared to that of the unsupported materials. Moreover, the structure of the reused catalyst remained the same as that of the fresh catalyst, indicating that the developed catalyst was structurally stable under reaction conditions.

The structural changes of the catalyst before and after use were further characterized using Fourier transform infrared spectroscopy (Fig. 4). Strong absorption peaks were observed in the range of 3000 to 4000  $cm^{-1}$  for both fresh and recovered catalysts, which might be assigned to the adsorption of  $-NH_2$  groups and partially to the stretching vibration of Al–O–K groups.<sup>25</sup> The presence of K–O–Al bonds implied the interaction between the active component and  $Al_2O_3$ , which may be one reason for the fine stability of the supported catalyst. Besides, the vibration of C–H in the methoxy substances at 2931 and 2961  $cm^{-1}$  were found on 14

Table 2 Physicochemical properties of the catalysts

Catalyst	$S_{BET}$ ( $m^2 g^{-1}$ )	$d_p^a$ (nm)	$v_p^b$ ( $cm^3 g^{-1}$ )	Amount of basic site <sup>c</sup> (mmol $g^{-1}$ )		
				Weak	Moderate	Total
KATriz	—	—	—	0.13	0.81	0.94
$Al_2O_3$	155.77	9.56	0.40	0.14	0.45	0.59
7 wt% KATriz/ $Al_2O_3$	218.29	9.60	0.54	0.34	0.54	0.88
14 wt% KATriz/ $Al_2O_3$	197.85	9.62	0.47	0.68	0.79	1.47
20 wt% KATriz/ $Al_2O_3$	153.51	9.56	0.40	0.61	0.42	1.03
14 wt% KATriz/ $Al_2O_3$ -reused	218.74	9.60	0.51	0.57	0.67	1.24

<sup>a</sup> Average pore size. <sup>b</sup> Average pore volume. <sup>c</sup> Determined by TPD.



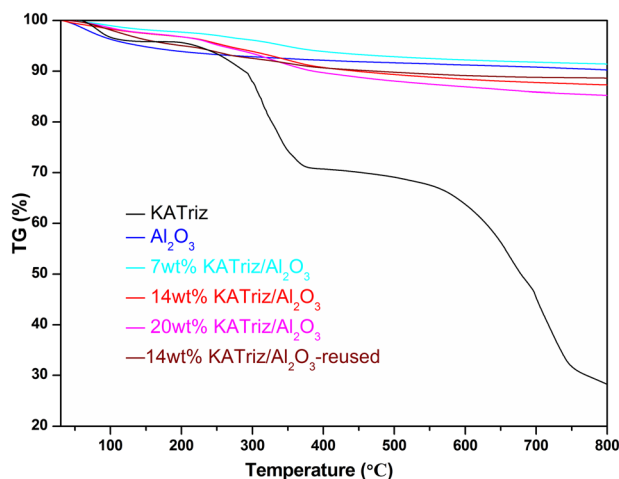


Fig. 2 TGA curve of KATriz,  $\text{Al}_2\text{O}_3$ , and KATriz/ $\text{Al}_2\text{O}_3$  catalysts.

wt% KATriz/ $\text{Al}_2\text{O}_3$ -reused.<sup>26,27</sup> In addition, the absorption peaks of C=O and C-O-C were also detected at  $1724\text{ cm}^{-1}$  and  $1270\text{ cm}^{-1}$ , respectively, on the recovered catalyst, which should be the carbonate species adsorbed on the catalyst surface,<sup>28</sup> and the results are in accordance with the TG analyses. The IR results indicated that only the reaction raw materials or products were adsorbed on the surface of the catalyst, and no obvious change was observed in the structure of the reused catalyst.

XPS was used to determine the surface chemical state and composition of each element on 14 wt% KATriz/ $\text{Al}_2\text{O}_3$  catalysts (Fig. 5a). In KATriz salt, K 2p (Fig. 5b) peaks at 292.8 eV and 295.6 eV belonged to K  $2p_{3/2}$  and K  $2p_{1/2}$ , and after loading KATriz on  $\text{Al}_2\text{O}_3$ , the binding energy of K 2p increased to 293.0 eV and 295.8 eV, respectively. In the  $\text{Al}_2\text{O}_3$  carrier, the binding energy of Al 2p (Fig. 5c) corresponded to Al oxide at 74.5 eV. On the contrary, the binding energy of Al 2p decreased by approximately 0.2 eV. This might be because the

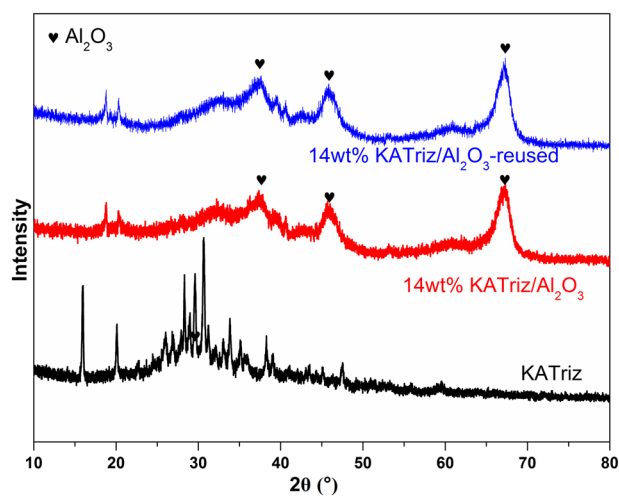


Fig. 3 XRD patterns of KATriz, 14 wt% KATriz/ $\text{Al}_2\text{O}_3$  and 14 wt% KATriz/ $\text{Al}_2\text{O}_3$ -reused.

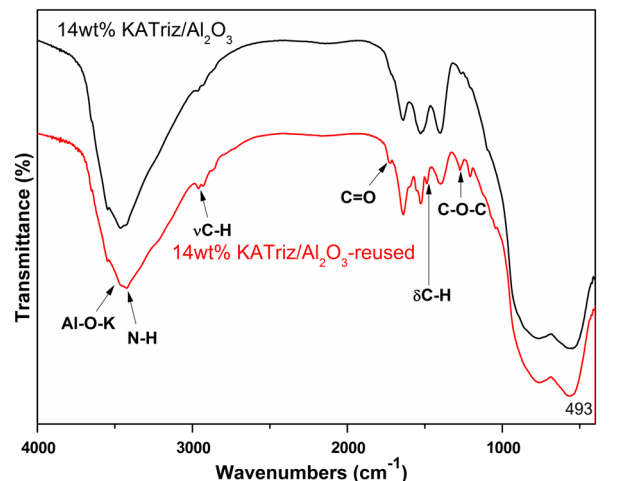


Fig. 4 IR spectra of 14 wt% KATriz/ $\text{Al}_2\text{O}_3$  and 14 wt% KATriz/ $\text{Al}_2\text{O}_3$ -reused.

electronegativity of Al was stronger than that of K. After loading with KATriz, electrons around  $\text{K}^+$  transferred to  $\text{Al}^{3+}$ , resulting in an increase in  $\text{Al}^{3+}$  electron density and a decrease in  $\text{K}^+$  electron density, indicating a weak interaction between KATriz and  $\text{Al}_2\text{O}_3$ .<sup>18</sup> The interaction between the active component KATriz and  $\text{Al}_2\text{O}_3$  had a critical impact on the performance and stability of the catalyst. This interaction not only improved the activity of catalytic reactions but also enhanced the selectivity and lifetime of 14 wt% KATriz/ $\text{Al}_2\text{O}_3$ . This may be one reason why the loaded catalyst (14 wt% KATriz/ $\text{Al}_2\text{O}_3$ ) expressed higher activity and stability than KATriz salt. The O 1s peak (Fig. 5d) exhibited three typical XPS peaks at 530.3, 531.4, and 532.7 eV, which are attributed to lattice oxygen, oxygen defects, and surface adsorbed oxygen species, respectively.<sup>29,30</sup> The N 1s peak (Fig. 5e) could be divided into three peaks (398.5, 399.4, and 400.7 eV).<sup>31–33</sup> The peaks at 398.5 eV and 399.4 eV are associated with two types of N on the triazole ring, and the peak at 400.7 eV could be assigned to  $-\text{NH}_2$  nitrogen (401.1–403.6 eV). The peaks of C 1s (Fig. 5f) are divided into three peaks: 284.3 eV, 285.0 eV and 286.2 eV. The peak at 286.2 eV corresponds to  $\text{sp}^2$ -type carbon such as the C=N groups, and the carbon in triazole. The peak at 285.0 eV corresponds to C-N and the peak at 284.3 eV indicates C-C groups.<sup>31–33</sup>

According to the TG analyses, the decomposition temperature of KATriz salt was about 300 °C. To avoid the effect caused by KATriz salt decomposition, the desorption temperature was set as 300 °C and it was maintained until the signal returned to baseline. The  $\text{CO}_2$ -TPD spectra (Fig. 6) revealed that there were two main peaks for the KATriz/ $\text{Al}_2\text{O}_3$  catalysts, which could be divided into weak basic sites (<200 °C) and medium basic sites (200–300 °C). It could be seen that KATriz salt and  $\text{Al}_2\text{O}_3$  support owned a smaller number of weak basic sites. For KATriz/ $\text{Al}_2\text{O}_3$  catalysts with different loading amounts, the peak center shifted to a higher temperature as the content of KATriz was augmented. The desorption temperatures were 74 °C, 102 °C and 122 °C for 7 wt%, 14 wt%, and 20 wt% KATriz/ $\text{Al}_2\text{O}_3$ , respectively. The amounts of basic sites were



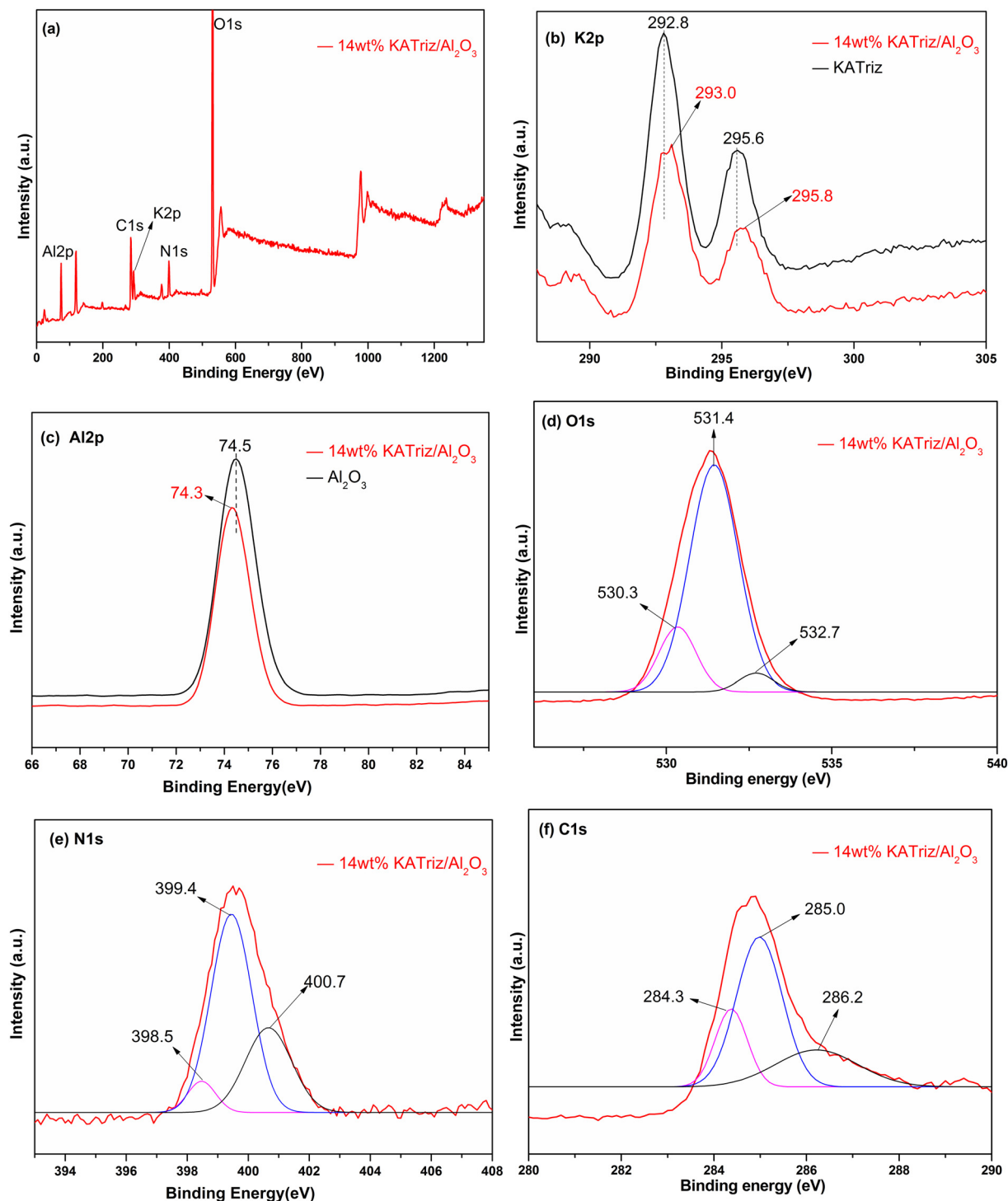


Fig. 5 XPS survey spectra: (a) 14 wt% KATriz/ $\text{Al}_2\text{O}_3$ ; (b) K 2p peaks; (c) Al 2p peaks; (d) O 1s peaks; (e) N 1s peaks and (f) C 1s peaks.

calculated from the desorption amounts of  $\text{CO}_2$  (Table 2, Fig. S1†). The number of weakly basic sites increased firstly and then decreased with the increase of the KATriz content, reaching the maximum when the loading amount was 14 wt% (0.68 mmol  $\text{CO}_2$  per g). The amount decreased to 0.61 mmol  $\text{CO}_2$  per g as the KATriz loading was elevated to 20 wt%. Moreover, all catalysts exhibited broad desorption peaks at

around 300 °C, belonging to medium basic sites. KATriz salt displayed the highest medium basic sites and the relatively lower weak basic sites; while the weak basic sites heightened after loading on  $\text{Al}_2\text{O}_3$ , which might be due to the emerging new surface structure as conjectured from the BET results. The regularity of the number of medium basic sites for the supported catalysts was the same as that of weak basic sites.



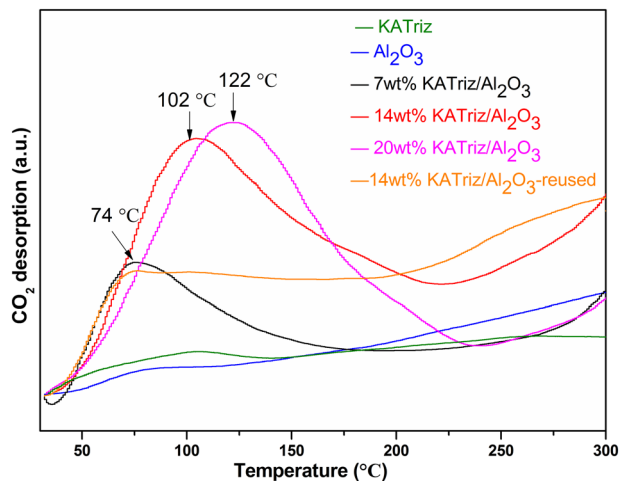


Fig. 6 CO<sub>2</sub>-TPD profiles of KATriz, Al<sub>2</sub>O<sub>3</sub>, and KATriz/Al<sub>2</sub>O<sub>3</sub> catalysts.

The number of weak and medium basic sites first increased and then decreased with the increase of KATriz content, which might be due to the destruction of the pore structure shown by BET results or the overlapping effect of the excessive KATriz.<sup>13</sup> Additionally, the basic sites in the reused catalyst also decreased, which was caused by the loss of small amounts of active components. The total number of basic sites was in the following order: 14 wt% KATriz/Al<sub>2</sub>O<sub>3</sub> (1.47 mmol CO<sub>2</sub> per g) > 20 wt% KATriz/Al<sub>2</sub>O<sub>3</sub> (1.04 mmol CO<sub>2</sub> per g) > KATriz (0.94 mmol CO<sub>2</sub> per g) > 7 wt% KATriz/Al<sub>2</sub>O<sub>3</sub> (0.88 mmol CO<sub>2</sub> per g) > Al<sub>2</sub>O<sub>3</sub> (0.59 mmol CO<sub>2</sub> per g). Based on the quantitative results of CO<sub>2</sub>-TPD and the catalytic performance of the catalyst used, the yield of DEC was consistent with the total number of basic sites.

### 3.2 Catalysts for the transesterification of DMC

The catalytic performance of various catalysts for the transesterification of DMC with C<sub>2</sub>H<sub>5</sub>OH is listed in Table 3. Obviously, the conversion of DMC was very low without a

catalyst (entry 1). When Al<sub>2</sub>O<sub>3</sub> was used as a catalyst (entry 2), the conversion of DMC slightly increased to 24%, the main product was EMC with a selectivity of 89%. The reaction with neat KATriz (entry 3) showed higher activity (80% DMC conversion and 87% DEC selectivity) compared to that with Al<sub>2</sub>O<sub>3</sub>. The KATriz/Al<sub>2</sub>O<sub>3</sub> catalysts with different KATriz contents were then tested on the transesterification reaction between DMC and C<sub>2</sub>H<sub>5</sub>OH (entries 4–6). The conversion of DMC first increased and then decreased with the increase of KATriz content, and 14% wt KATriz/Al<sub>2</sub>O<sub>3</sub> showed the highest activity, with 88% DMC conversion and 91% DEC selectivity. According to the analysis of XRD, BET and TPD results, the good dispersibility of KATriz on Al<sub>2</sub>O<sub>3</sub> increased the specific surface area and the number of basic sites of the supported catalyst, which might be the reason why 14 wt% KATriz/Al<sub>2</sub>O<sub>3</sub> showed better activity than KATriz. Moreover, the good dispersibility of KATriz on Al<sub>2</sub>O<sub>3</sub> could reduce the usage of active components. The activity of the synthesized KATriz/Al<sub>2</sub>O<sub>3</sub> catalysts was related to the alkalinity of the catalysts, supplied by KATriz. Also, the conversions of DMC on these KATriz/Al<sub>2</sub>O<sub>3</sub> catalysts were basically consistent with the total amounts of basic sites. Moreover, the BET results indicated that the high loading of KATriz (20 wt%) leads to a decrease in the pore volume and surface area, which might be ascribed to the aggregation of KATriz on the catalyst surface. By using catalyst 14 wt% KATriz/Al<sub>2</sub>O<sub>3</sub> and extending the reaction time to 24 h, the selectivity of DEC reached a maximum of 99%, but the conversion of DMC slightly increased from 88% to 90% (entry 7). The stability of the catalysts is an important parameter determining their applicability in practical applications. Therefore, KATriz/Al<sub>2</sub>O<sub>3</sub> was recycled through filtration and reused without any treatment. The conversion of DMC was basically maintained for the reused catalyst, and the selectivity of DEC decreased to 80% (entries 8–10). Although the activity decreased during the first repeated use, it remained basically unchanged during the 3rd and 4th runs, suggesting that the catalyst was stable and the catalytic activity could be basically maintained.

Table 3 Performances of various catalysts in the transesterification of DMC to DEC<sup>a</sup>

Entry	Catalyst	DMC : C <sub>2</sub> H <sub>5</sub> OH molar ratio	DMC conversion (%)	Selectivity (%)	
				EMC	DEC
1	—	1 : 10	14	79	21
2	Al <sub>2</sub> O <sub>3</sub>	1 : 10	24	89	11
3	KATriz	1 : 10	80	13	87
4	7 wt% KATriz/Al <sub>2</sub> O <sub>3</sub>	1 : 10	63	64	36
5	14 wt% KATriz/Al <sub>2</sub> O <sub>3</sub>	1 : 10	88	9	91
6	20 wt% KATriz/Al <sub>2</sub> O <sub>3</sub>	1 : 10	89	10	90
7 <sup>b</sup>	14 wt% KATriz/Al <sub>2</sub> O <sub>3</sub>	1 : 10	90	1	99
8	14 wt% KATriz/Al <sub>2</sub> O <sub>3</sub> -2nd run	1 : 10	86	19	81
9	14 wt% KATriz/Al <sub>2</sub> O <sub>3</sub> -3rd run	1 : 10	85	20	80
10	14 wt% KATriz/Al <sub>2</sub> O <sub>3</sub> -4th run	1 : 10	86	21	79
11 <sup>c</sup>	14 wt% KATriz/Al <sub>2</sub> O <sub>3</sub>	2 : 1	40	95	5
12 <sup>c</sup>	14 wt% KATriz/Al <sub>2</sub> O <sub>3</sub>	3 : 1	19	98	2
13 <sup>c</sup>	14 wt% KATriz/Al <sub>2</sub> O <sub>3</sub>	4 : 1	14	99	1

<sup>a</sup> Reaction conditions: 10 mmol DMC, 100 mmol ethanol, 100 mg catalyst, 80 °C, 8 h. <sup>b</sup> 24 h. <sup>c</sup> 30 mmol DMC.



Compared with fresh catalysts, the decrease in activity may be due to the loss of the active component KATriz on the catalyst surface during the reaction process. This can be seen from the TPD and BET results that the alkalinity of the catalyst decreased and the specific surface area increased.

In addition, the synthesis of EMC under different DMC and ethanol ratios was also investigated using 14 wt% KATriz/Al<sub>2</sub>O<sub>3</sub>. When the molar ratio of DMC to ethanol was 2:1, the conversion of DMC was 40%, with 95% selectivity of EMC. As DMC:ethanol = 3:1, the conversion of DMC was 19%, and the selectivity of EMC was 98%. Further increasing the amount of DMC until DMC:ethanol = 4:1, the selectivity of EMC could be up to 99%. Although adding the amount of DMC would improve the selectivity of EMC, the corresponding conversion of DMC would also decrease. Therefore, in the later fixed bed investigation, we fixed the ratio of DMC to ethanol at 2:1.

### 3.3 Optimization of the reaction conditions in the kettle mode

Firstly, the influence of the temperature ranging between 50–90 °C is depicted in Fig. 7a. Both DMC conversion and DEC selectivity increased observably when the reaction temperature rose from 50 °C (25% DMC conversion and 12.6% DEC selectivity) to 80 °C (88% DMC conversion and 91% DEC selectivity), suggesting that the reaction temperature had a significant influence on the DEC synthesis. However, further increasing the reaction temperature to 90 °C did not obviously improve the DMC conversion and the DEC selectivity. During the heating process from 50–90 °C, the selectivity of EMC gradually decreased, indicating that high temperature contributed to the conversion rate of EMC to DEC.

Then, the effect of the C<sub>2</sub>H<sub>5</sub>OH/DMC molar ratio on DEC synthesis was examined (Fig. 7b). While the DMC conversion and DEC selectivity increased by raising the C<sub>2</sub>H<sub>5</sub>OH/DMC ratio from 2 to 10, and reached its maximum value for a C<sub>2</sub>H<sub>5</sub>OH/DMC ratio equal to 10 (88% DMC conversion and 91.5% DEC selectivity); in order to eliminate the effect caused by concentration, the catalyst dosage was increased to 0.12 g and 0.15 g when the ethanol to DMC ratio was 12 and 15, respectively. However, further increasing the molar ratio to 15, the selectivity of DEC was greatly reduced again. This may be because the concentration of DMC and the formed EMC declined as the molar ratio of C<sub>2</sub>H<sub>5</sub>OH/DMC was too high; leading to the fact that intermediate EMC could not be converted to DEC quickly in a given reaction time. From the practical viewpoint, the suitable molar ratio of C<sub>2</sub>H<sub>5</sub>OH/DMC was 10 for DEC.

Also, the effect of the reaction time on this transesterification reaction was explored (Fig. 7c). Obviously, increasing time had a beneficial impact on DMC conversion. The conversion rate of DMC was very fast within the first two hours, and then gradually decreased with the extension of reaction time. In the initial 30 min of the reaction, the conversion of DMC was low, but the selectivity of EMC was as

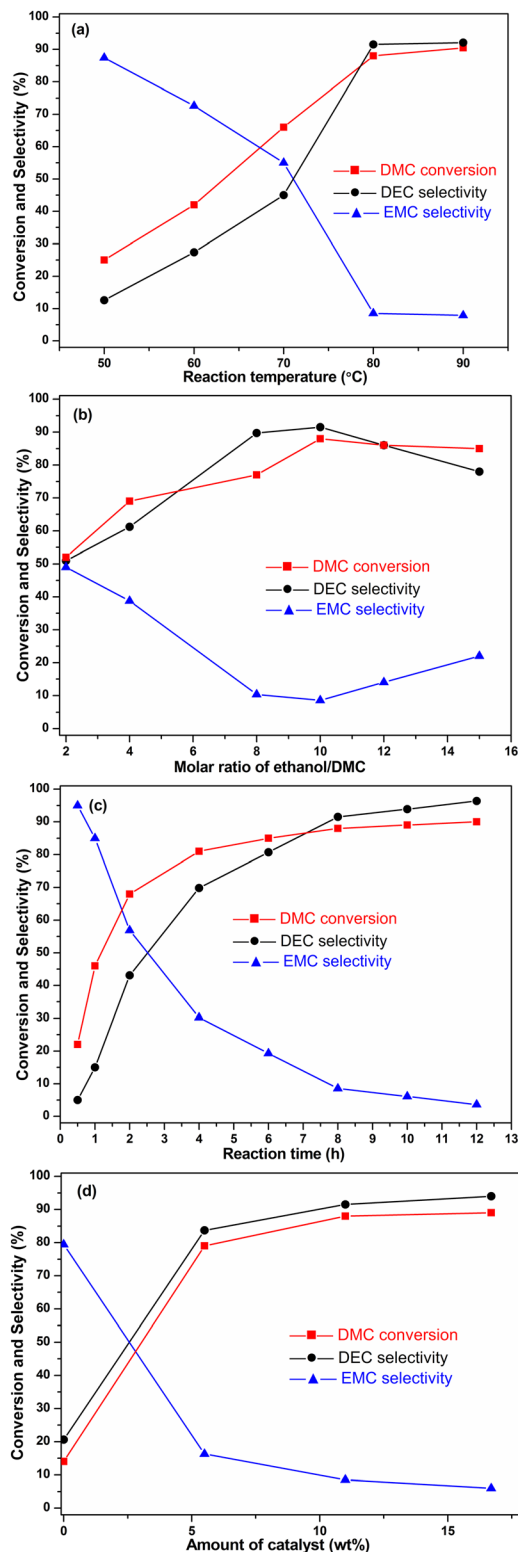


Fig. 7 Transesterification reaction of DMC with C<sub>2</sub>H<sub>5</sub>OH on the 14 wt% KATriz/Al<sub>2</sub>O<sub>3</sub> catalyst at different conditions. (a) Effect of reaction temperature: 10 mmol DMC, 100 mmol C<sub>2</sub>H<sub>5</sub>OH, 0.1 g 14 wt% KATriz/Al<sub>2</sub>O<sub>3</sub>, 8 h; (b) effect of the C<sub>2</sub>H<sub>5</sub>OH/DMC molar ratio: 0.1 g 14 wt% KATriz/Al<sub>2</sub>O<sub>3</sub>, 80 °C, 8 h (the catalyst dosage was increased to 0.12 g and 0.15 g when the ethanol to DMC ratio was 12 and 15, respectively); (c) effect of reaction time: 10 mmol DMC, 100 mmol C<sub>2</sub>H<sub>5</sub>OH, 0.1 g 14 wt% KATriz/Al<sub>2</sub>O<sub>3</sub>, 80 °C; (d) effect of amount of catalyst: 10 mmol DMC, 100 mmol C<sub>2</sub>H<sub>5</sub>OH, 80 °C, 8 h.



high as 95%, and the selectivity of DEC was 5%. As the reaction time prolonged, the selectivity of EMC gradually declined; on the contrary, the selectivity of DEC increased. The results showed that the EMC was first formed from DMC and  $C_2H_5OH$ , as EMC concentration reached a certain value, it would be converted to DEC. EMC was an intermediate in the synthesis of DEC through the transesterification reaction between DMC and  $C_2H_5OH$ . Considering that DEC was the target product, the optimal reaction time was 8 h.

Finally, the amount of the catalyst charged on DEC synthesis is shown in Fig. 7d. Both conversion and selectivity improved with the increase of the catalyst loading of 14 wt% KATriz/ $Al_2O_3$  till the amounts of the charged catalyst was 11 wt%, and further increment of the catalyst loading did not enhance the catalytic performance. Therefore, the 14 wt% KATriz/ $Al_2O_3$  dosage of 11 wt% was appropriate.

### 3.4 EMC syntheses in fixed bed mode

Based on the good yield achieved in the kettle mode, we further investigated the reaction between DMC and ethanol for EMC in a continuous flow mode. The activity of the 14 wt% KATriz/ $Al_2O_3$  catalyst *versus* weight hourly space velocity (WHSV) was tested with a molar ratio of DMC to ethanol of 1:2 (Fig. 8). It could be seen that both the conversion of DMC and selectivity of DEC reduced as the WHSV increased from 0.6 to 6.0  $h^{-1}$ . The DMC conversion, EMC selectivity and DEC selectivity were 68%, 75% and 25%, respectively, as the WHSV was 0.6  $h^{-1}$ . While, they declined to 35%, 85%, and 15%, respectively, when the WHSV was raised to 6  $h^{-1}$ . These results suggested that WHSV is an important factor in the activity of the tested catalysts.

Fig. 9 shows the activity of 14 wt% KATriz/ $Al_2O_3$  under different molar ratios of DMC to  $C_2H_5OH$ . As the molar ratio of DMC to ethanol increased from 1:2 to 2:1, the selectivity of EMC increased from 75% to 93%, while the corresponding

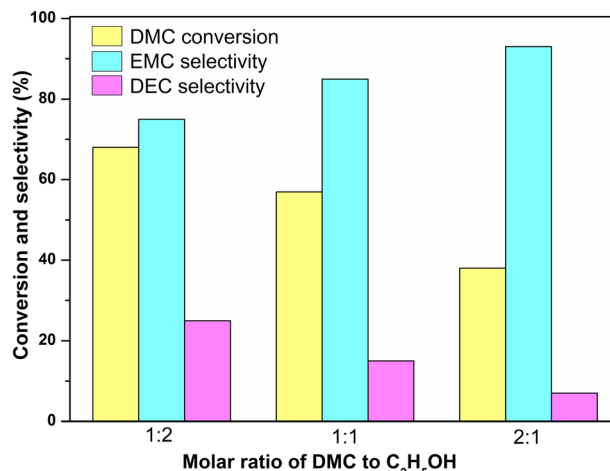


Fig. 9 Transesterification reaction of DMC with ethanol at different molar ratios of DMC to  $C_2H_5OH$ . (reaction conditions: 80 °C and WHSV = 0.9  $h^{-1}$ ).

conversion of DMC decreased from 68% to 38%, respectively. Although further increasing the amount of DMC would improve EMC selectivity, the actual production capacity may decrease. Therefore, it is necessary to balance the relationship between the production capacity and selectivity in the actual production process. Thus, DMC/ $C_2H_5OH$  = 2 was the relatively reasonable choice for obtaining high EMC selectivity and DMC conversion. The supported 14 wt% KATriz/ $Al_2O_3$  catalyst could also remain stable after a time on stream of 500 h (Fig. 10). Under the conditions of 80 °C, DMC/ethanol = 2 (molar ratio), and LHSV = 0.6  $h^{-1}$ , the conversion rate of ethanol was maintained at about 45%, and the selectivity of EMC was around 92%. To further verify the stability of the catalyst, the reaction was carried out at a higher LHSV (6  $h^{-1}$ ) for 24 h (Fig. S2†). Some physically adsorbed active components on the catalyst surface were lost

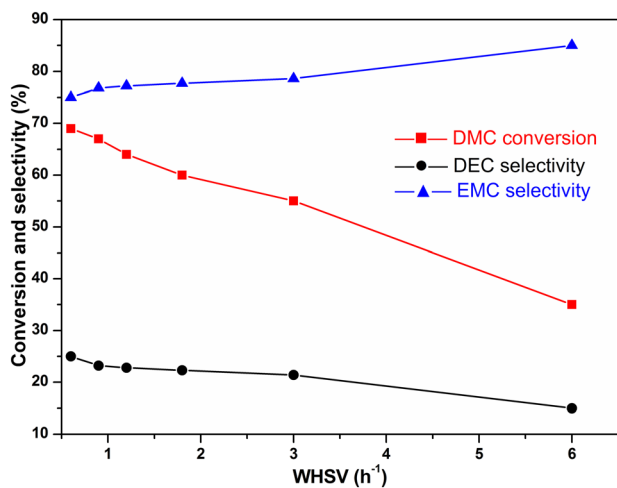


Fig. 8 Transesterification reaction of DMC with ethanol at different WHSV [reaction conditions: 80 °C and ethanol/DMC = 2 (mol ratio)].

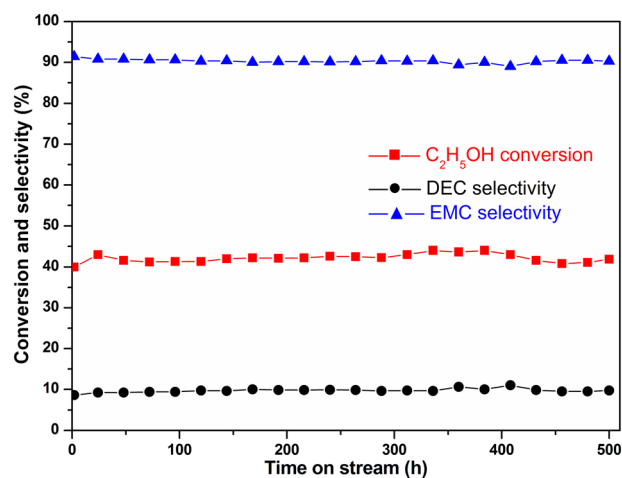


Fig. 10 Stability of the 14 wt% KATriz/ $Al_2O_3$  catalyst for the transesterification of DMC and  $C_2H_5OH$  [reaction conditions: 80 °C, DMC/ethanol = 2 (molar ratio), and LHSV = 0.6  $h^{-1}$ ].



at high flow rates, resulting in a decrease in the catalyst activity in the early stage, but it could remain stable in the later stage.

## 4. Conclusions

KATriz/Al<sub>2</sub>O<sub>3</sub> catalyst was developed and tested for the transesterification reaction between DMC and ethanol under both kettle-type reaction and fixed bed conditions. The introduction of an appropriate amount of active component KATriz significantly increased the specific surface area and alkaline sites in the Al<sub>2</sub>O<sub>3</sub> support, which also improved the dispersion and stability of KATriz active sites. The favourable catalytic performance stemmed from the synergistic effect between the alkaline KATriz and Al<sub>2</sub>O<sub>3</sub>. Besides, KATriz/Al<sub>2</sub>O<sub>3</sub> also showed fine stability and might be an effective catalyst for syntheses of DEC and EMC *via* transesterification.

## Data availability

The data supporting this article have been included as part of the ESI.†

## Conflicts of interest

There are no conflicts to declare.

## Acknowledgements

This work was supported by Shandong Energy Institute (SEI U202321), National Natural Science Foundation of China (No. U22A20393, 21925207), LICP Cooperation Foundation for Young Scholars (HZJJ22-07), the Major Project of Gansu Province, China (23JRRA603, 22ZD6GA003, 21ZD4WA021).

## Notes and references

- S. Huang, B. Yan, S. Wang and X. Ma, *Chem. Soc. Rev.*, 2015, **44**, 3079–3116.
- Y. Wang, S. Wang, Y. Zhang, P. Lee and D. Y. W. Yu, *ACS Appl. Energy Mater.*, 2019, **2**, 7512–7517.
- P. Tundo, M. Musolino and F. Aricò, *Green Chem.*, 2018, **20**, 28–85.
- A.-A. G. Shaikh and S. Sivaram, Organic carbonates, *Chem. Rev.*, 1996, **96**, 951–976.
- S. Huang, P. Chen, B. Yan, S. Wang, Y. Shen and X. Ma, *Ind. Eng. Chem. Res.*, 2013, **52**, 6349–6356.
- H. Xiong, W. Mo, J. Hu, R. Bai and G. Li, *Ind. Eng. Chem. Res.*, 2009, **48**, 10845–10849.
- F. Mei, E. Chen and G. Li, *Kinet. Catal.*, 2009, **50**, 666–670.
- F. Mei, E. Chen and G. Li, *React. Kinet. Catal. Lett.*, 2009, **96**, 27–33.
- Y. Yu, L. Shi, J. Guo, X. Li, W. Yang, Z. Zhang and G. Xu, *Fuel*, 2021, **285**, 119201.
- I. Zielinska-Nadolska, K. Warmuzinski and J. Richter, *Catal. Today*, 2006, **114**, 226–230.
- L. Desidery, S. Chaemcheun, M. Yusubov and F. Verpoort, *Catal. Commun.*, 2018, **104**, 82–85.
- C. Murugan and H. C. Bajaj, *Fuel Process. Technol.*, 2011, **92**, 77–82.
- C. Liu, Z. Chi, Y. Yan, Z. Lu, X. Li, J. Yan, M. Luo and W. Xiao, *Ind. Eng. Chem. Res.*, 2023, **62**, 1264–1276.
- F. Mei, E. Chen, G. Li and A. Zhang, *React. Kinet. Catal. Lett.*, 2008, **93**, 101–108.
- J. Lv, H. Cai, Y. Guo, W. Liu, N. Tao, H. Wang and J. Liu, *ChemistrySelect*, 2019, **4**, 7366–7370.
- H. Wang, W. Liu, Y. Wang, N. Tao, H. Cai, J. Liu and J. Lv, *Ind. Eng. Chem. Res.*, 2020, **59**, 5591–5600.
- Z. Qi, S. Li, Y. Cai, R. Cui, J. Chen, C. Ye and T. Qiu, *Fuel*, 2023, **334**, 126659.
- P. Yan, X. Zhang, Y. Huang, G. Liu, P. Liu, C. Li, P. Pan and Y. Yao, *ChemistrySelect*, 2023, **8**, e202203952.
- M. Trueba and S. P. Trasatti, *Eur. J. Inorg. Chem.*, 2005, **2005**, 3393–3403.
- A. Islam, Y. H. Taufiq-Yap, P. Ravindra, S. H. Teo, S. Sivasangar and E.-S. Chan, *Energy*, 2015, **89**, 965–973.
- R. Bai, Y. Wang, S. Wang, F. Mei, T. Li and G. Li, *Fuel Process. Technol.*, 2013, **106**, 209–214.
- S. Baroutian, M. K. Aroua, A. A. A. Raman and N. M. N. Sulaiman, *Fuel Process. Technol.*, 2010, **91**, 1378–1385.
- P. Wang, Y. Fei, Q. Li and Y. Deng, *Green Chem.*, 2016, **18**, 6681–6686.
- P. Cao, H. Zhao, S. Adegbite, B. Yang, E. Lester and T. Wu, *Fuel*, 2021, **298**, 120599.
- W. Xie and H. Li, *J. Mol. Catal. A: Chem.*, 2006, **255**, 1–9.
- A. Khaleel, M. Ahmed and S. B. Sowaid, *Colloids Surf., A*, 2019, **571**, 174–181.
- V. Piazza, R. B. S. Junior, G. Luccisano, D. Pietroggiacomini, G. Groppi, D. Gazzoli and A. Beretta, *J. Catal.*, 2022, **413**, 184–200.
- Y. Gao, Z. Li, K. Su and B. Cheng, *Chem. Eng. J.*, 2016, **301**, 12–18.
- D. Mishra, B. P. Mandal, R. Mukherjee, R. Naik, G. Lawes and B. Nadgorny, *Appl. Phys. Lett.*, 2013, **102**, 182404.
- J.-C. Dupin, D. Gonbeau, P. Vinatier and A. Levasseur, *Phys. Chem. Chem. Phys.*, 2000, **2**, 1319–1324.
- R. Arrigo, M. S. Havecker, S. Wrabetz, R. Blume, M. Lerch, J. McGregor, E. P. J. Parrott, J. A. Zeitler, L. F. Gladden, A. Knop-Gericke, R. Schlogl and D. S. Su, *J. Am. Chem. Soc.*, 2010, **132**, 9616–9630.
- K. Jurewicz and K. Babel, *Energy Fuels*, 2010, **24**, 3429–3435.
- X. Yuan, M. Zhang, X. Chen, N. An, G. Liu, Y. Liu, W. Zhang, W. Yan and M. Jia, *Appl. Catal., A*, 2012, **439–440**, 149–155.

